

## Research Note

# Fluorescence Lifetime Spectroscopy of Glioblastoma Multiforme<sup>¶</sup>

Laura Marcu<sup>\*1,2,3</sup>, Javier A. Jo<sup>1</sup>, Pramod V. Butte<sup>1,2</sup>, William H. Yong<sup>4</sup>, Brian K. Pikul<sup>5</sup>, Keith L. Black<sup>5</sup> and Reid C. Thompson<sup>6</sup>

<sup>1</sup>Biophotonics Research and Technology Development Laboratory, Department of Surgery, Cedars-Sinai Medical Center, Los Angeles, CA

<sup>2</sup>Department of Biomedical Engineering, University of Southern California, Los Angeles, CA

<sup>3</sup>Department of Electrical Engineering, University of Southern California, Los Angeles, CA

<sup>4</sup>Department of Pathology and Laboratory Medicine, Cedars-Sinai Medical Center, Los Angeles, CA

<sup>5</sup>Maxine Dunitz Neurosurgical Institute, Cedars-Sinai Medical Center, Los Angeles, CA

<sup>6</sup>Department of Neurosurgery, Vanderbilt University Medical Center, Nashville, TN

Received 8 December 2003; accepted 12 April 2004

## ABSTRACT

Fluorescence spectroscopy of the endogenous emission of brain tumors has been researched as a potentially important method for the intraoperative localization of brain tumor margins. We investigated the use of time-resolved, laser-induced fluorescence spectroscopy for demarcation of primary brain tumors by studying the time-resolved spectra of gliomas. The fluorescence of human brain samples (glioblastoma multiforme, cortex and white matter: six patients, 23 sites) was induced *ex vivo* with a pulsed nitrogen laser (337 nm, 3 ns). The time-resolved spectra were detected in a 360–550 nm wavelength range using a fast digitizer and gated detection. Parameters derived from both the spectral- (intensities from narrow spectral bands) and the time domain (average lifetime) measured at 390 and 460 nm were used for tissue characterization. We determined that high-grade gliomas are characterized by fluorescence lifetimes that varied with the emission wavelength (>3 ns at 390 nm, <1 ns at 460 nm) and their emission is overall longer than that of normal brain tissue. Our study demonstrates that the use of fluorescence lifetime not only improves the specificity of fluorescence measurements but also allows a more robust evaluation of data collected from brain tissue. Combined information from both the spectral- and the time domain can enhance the ability of fluorescence-based techniques to diagnose and detect brain tumor margins intraoperatively.

## INTRODUCTION

Despite aggressive treatment including surgical resection, irradiation and chemotherapy, the median survival of patients diagnosed with malignant gliomas is less than 1 year. The extent of surgical resection is a primary determinant of the outcome in patients diagnosed with malignant glioma. Gross total resection is associated with longer survival and improved neurologic function (1). Patients undergoing resection of malignant glioma using image-guided navigation techniques, wherein computer tomography or magnetic resonance imaging facilitates an “image complete” resection, have a median survival of about 70 weeks (2,3). This is in stark contrast to those patients who have a subtotal resection or biopsy, in whom median survival is less than 19 weeks. Currently, the degree to which a complete resection can be achieved in the brain is limited by a number of factors unique to the central nervous system. The extent of resection is limited primarily by the difficulty in visually detecting differences between normal brain and malignant tissue during surgery. Thus, patients with malignant gliomas often have a subtotal resection. In addition, patients may experience neurological morbidity if the resection is inadvertently carried into normal brain tissue. Because outcome is closely related to the extent of surgical resection, and the degree of resection is limited by difficulties in visually differentiating tumor from normal brain, there is a pressing need to develop new strategies to improve the intraoperative imaging of malignant glioma.

Fluorescence spectroscopy of tissues offers a potential method for intraoperative localization of tumor margins, diagnosis of neoplasms and optimization of biopsy and therapeutic procedures (4–6). It has been shown that intracranial tumors including primary brain tumors can be distinguished from normal brain tissue on the basis of their autofluorescence emission spectra (7–11). Studies were performed on *ex vivo* brain specimens (8,9) as well as *in vivo* in patients undergoing resection of brain tumors (7,11). However, these studies have not fully explored or demonstrated the potential use of fluorescence spectroscopy as a clinical tool for intraoperative delineation of these tumors. The time dependence of emission and the potential information contained therein can improve the specificity of fluorescence measurement (12–16). What is lacking

<sup>¶</sup>Posted on the website on 6 May 2004

\*To whom correspondence should be addressed: Biophotonics Research and Technology Development Laboratory, Department of Surgery, 8700 Beverly Boulevard, Davis Building G149A, Cedars-Sinai Medical Center, Los Angeles, CA 90048, USA. Fax: 310-423-8414; e-mail: lmarcu@bmsrs.usc.edu

Abbreviations: GBM, glioblastoma multiforme; FIRF, fluorescence impulse response function; NAD(P)H, reduced nicotinamide adenine dinucleotide (phosphate); TR-LIFS, time-resolved, laser-induced fluorescence spectroscopy.

© 2004 American Society for Photobiology 0031-8655/04 \$5.00+0.00

for the application of this time-resolved technique is the detailed knowledge of the measurability of time-resolved spectra from brain tumors and tissues in question.

The overall objective of this work is to assess the diagnostic value of a fluorescence lifetime spectroscopy technique for intraoperative brain tumor delineation. As part of this ongoing work, we measured the time-resolved fluorescence emission of glioblastoma multiforme (GBM, Grade IV) *ex vivo* and identified characteristics of time-resolved fluorescence emission that distinguish the tumor from the surrounding normal tissues including gray and white matter.

## MATERIALS AND METHODS

**Samples.** Brain tumor specimens histopathologically diagnosed as GBM Grade IV based on the World Health Organization classification and adjacent normal gray matter (cerebral cortex) were obtained during craniotomy from six patients. The study was carried out with the approval of the Cedars-Sinai Institutional Review Board. Samples of normal white matter were obtained from one trauma patient. The specimens were immediately transported to the laboratory wrapped in cotton surgical gauze moistened in saline and spectroscopically investigated within 1–3 h after surgical removal. Spectroscopic data were collected from a total of 23 sites.

**Instrumentation.** The tissue specimens were spectroscopically investigated with a prototype time-resolved laser-induced fluorescence spectroscopy (TR-LIFS) apparatus. The experimental setup used a fast digitizer and gated detection and was similar to that described previously (16). The light from a pulsed nitrogen laser (wavelength: 337.1 nm, repetition rate: 10 Hz) was focused onto a custom-designed (17) fiber-optic probe (Polymicro Technologies LLC, Phoenix, AZ) and directed onto the sample from above. The probe consisted of a central illumination fiber (600  $\mu\text{m}$ ) tapered to a distal core (nominal numerical aperture determined by the taper ratio  $\sim 1:1.7$ ). The pulse width measured at the tip of the fiber was 3 ns full width at half maximum. The resulting fluorescence emission was collected by a fiber optic bundle (ring of 18 collection fibers of 200  $\mu\text{m}$  core size) and focused into a scanning monochromator. The distance between the illumination fiber and each collection fiber (center-to-center) was 0.64 mm. The fluorescence emission was detected with a gated multichannel plate photomultiplier tube (rise time: 0.3 ns, bandwidth: 1 GHz) placed at the monochromator exit slit. The photomultiplier output was amplified (rise time: 0.35 ns, bandwidth: 1 GHz) and the entire fluorescent pulse from a single excitation laser pulse recorded with a digital oscilloscope (bandwidth: 1 GHz, sampling frequency: 5 Gsamples/s). A long pass filter (WG345, Schott Glass, Mainz, Germany; transmittance at 337 nm  $< 20\%$ , at 360 nm = 90%) was placed at the exit of the monochromator to prevent most of the laser light reflected by the sample from reaching the detector.

**Spectroscopic analysis.** The fluorescence emission of each sample was scanned in the 360–510 nm range at 5 nm intervals. To assess the lifetime reproducibility, five consecutive measurements were acquired at 390 and 460 nm. The energy output of the laser was adjusted to 3  $\mu\text{J}/\text{pulse}$  (*i.e.* total energy delivered  $< 2.2 \text{ mJ}/\text{mm}^2$  per 250 s measurement). The time-integrated fluorescence (spectral emission) was computed from the measured fluorescence response pulses by integrating each pulse as a function of time for each wavelength. The constructed fluorescence spectra were corrected for background noise and normalized by dividing the fluorescence intensity at each emission wavelength by the peak fluorescence intensity.

**Histopathologic analysis.** After spectroscopic investigation, areas where fluorescence was recorded were marked with ink. Each sample was then fixed in 10% buffered formalin, and transversely oriented sections (4 mm thick) were cut from the marked areas. The sections were embedded in paraffin and stained with hematoxylin and eosin (HE). The histological sections were evaluated by light microscopy. The morphologic and pathologic features within the volume probed by the excitation light beam, as defined by the light beam spot size and penetration depth, were primarily used for sample classification. On the basis of previous reports (7), the  $1/e$  optical penetration depth for 337 nm excitation wavelength is estimated to be 200–250  $\mu\text{m}$ . After histological assessment, eight samples that showed morphological characteristics different from those investigated in this study, such as low-grade gliomas, were excluded.

**Data analysis.** The TR-LIFS data recorded from malignant brain tissue and normal tissue for this study were analyzed using the Laguerre deconvolution method (18). Using the fluorescence impulse response function (FIRF) estimated at each emission wavelength in each of the TR-LIFS

data sets, a time-resolved spectrum was constructed. The time-resolved spectrum represents the intrinsic fluorescence decay as a function of time for the different emission wavelengths. To characterize the dynamics of fluorescence decay, the average lifetime ( $\tau$ ) estimated as the interpolated time at which the FIRF decays to  $1/e$  of its maximum value was used. The time-integrated spectrum (conventional or steady-state spectrum) was also recovered by integrating each estimated FIRF as a function of time. The spectrum is characterized by discrete fluorescence intensities that showed the variation of fluorescence as a function of emission wavelength. To compare the different brain tissue types on the basis of their fluorescence emission characteristics, the ratio ( $I_{390}/I_{460}$ ) between the fluorescence intensity from narrow spectral bands centered around 390 nm (380–400 nm) and 460 nm (450–470 nm) was computed, and the average lifetimes around 390 nm ( $\tau_{390}$ ) and 460 nm ( $\tau_{460}$ ) were also extracted. For statistical purposes, one-way analysis of variance applied to the spectroscopic parameters ( $I_{390}/I_{460}$ ,  $\tau_{390}$ ,  $\tau_{460}$ ) was used to evaluate differences between brain tissue types on the basis of the fluorescence emission characteristics. The level of significance used was  $P < 0.05$ .

## RESULTS

### Histology

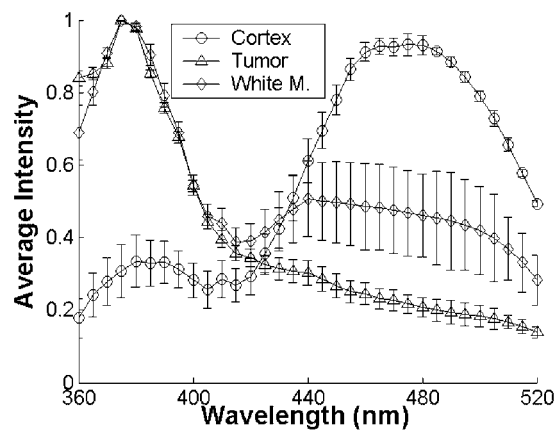
Of 23 sites that underwent spectroscopic examination, nine were classified as GBM, nine as normal cortex and five as normal white matter. GBM samples were characterized by robust infiltration of darkly stained polymorphic nuclei with atypia. A few samples showed the presence of subpial gliosis, mitosis, as well as endothelial proliferation, signifying Grade-IV glioma. Normal white matter was characterized by the presence of lightly stained axons and normal glial cells. Normal gray matter was characterized by the presence of pyramidal neurons with scattered small glial cells in pink neurophil background.

### Time-integrated fluorescence spectra

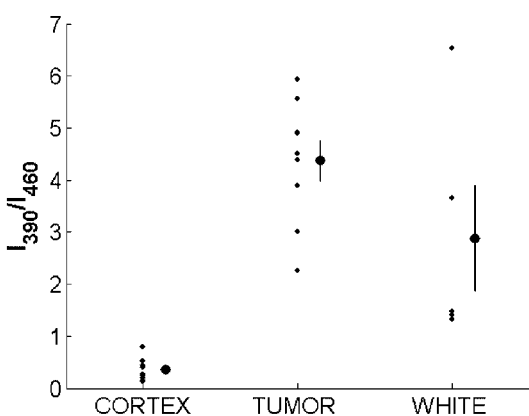
The time-integrated or steady-state spectra for each type of tissue are shown in Fig. 1a. The spectra from the cortex samples were characterized by a main peak between 460 and 480 nm and by a secondary peak around 380 nm. The white matter spectra presented a main peak at 380 nm and a secondary peak between 460 and 480 nm. In contrast, the tumor spectra showed a single peak around 380 nm. The ratio  $I_{390}/I_{460}$  of the spectral intensity values is shown in Fig. 1b. The ratios from the cortex sites were below unity, indicating the predominance of the peak at 460 nm over the peak at 390 nm. The ratios from the tumor sites were larger than 2, thus showing the predominance of the peak around 390 nm in the tumor spectra. In the case of the white matter spectra, three samples presented ratio values grouped between one and two, whereas the other two samples presented much higher ratio values. A variance test on the group samples showed that the  $I_{390}/I_{460}$  values for cortex were significantly lower relative to tumor ( $P < 0.001$ ). No significant differences were found, however, between the white matter and tumor  $I_{390}/I_{460}$  ratio.

### Time-resolved fluorescence spectra and fluorescence lifetimes

The time-resolved emission features of GBM were found to be distinct from those of the normal brain tissues, white matter and cortex. Typical FIRF of healthy and diseased brain tissue samples are shown in Fig. 2. The fluorescence decay dynamic of GBM and white matter was found to vary along the emission spectrum. The fluorescence lifetimes for each tissue type are depicted in Fig. 3. The lifetimes from the cortex (Fig. 3a) were generally below 1.5 ns and did not present major changes along the



a)

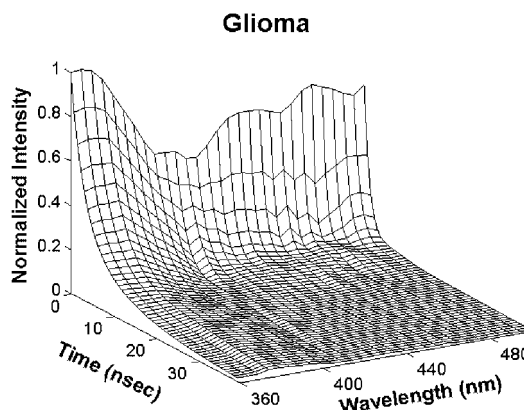


b)

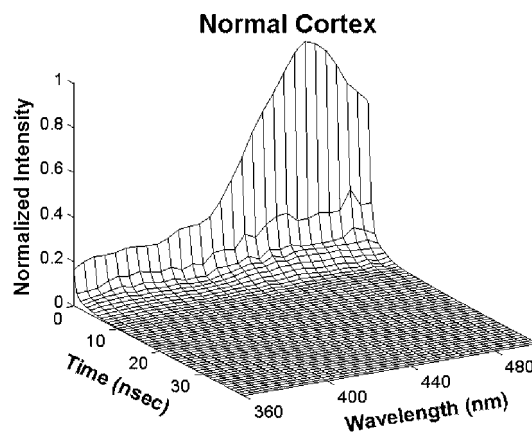
**Figure 1.** (a) Normalized fluorescence emission spectra of GBM, cortex and white matter. Results are depicted as mean  $\pm$  standard error of the data from each independent measurement. (b) The  $I_{390}/I_{460}$  ratio of each tissue type. Results are shown as mean  $\pm$  standard error of the data from each independent measurement.

entire wavelength range (e.g.  $\tau_{390} = 0.76 \pm 0.1$ ;  $\tau_{460} = 0.68 \pm 0.1$ ). The tumor samples presented long lifetimes (above 3 ns) at the blueshifted wavelengths ( $\tau_{390} = 4.05 \pm 0.26$ ), and as the wavelengths increased, the lifetime values decreased significantly ( $\tau_{460} = 1.03 \pm 0.1$ ). For white matter samples the lifetime values were centered at 2 ns ( $\tau_{390} = 2 \pm 0.8$ ), presented high variability (large SE) for wavelengths below 440 nm, whereas for longer wavelengths the lifetimes became shorter, below 1 ns ( $\tau_{460} = 0.69 \pm 0.08$ ), comparable with those measured in normal cortex.

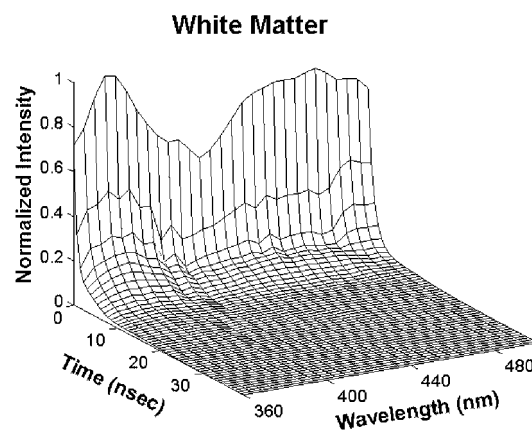
The lifetimes for the two regions of interest (around 390 and 460 nm) are shown in Fig. 3b,c. All  $\tau_{390}$  values from cortex sites were below 1.5 ns, whereas those from the tumor sites were above 2 ns. In the case of the white matter spectra, three samples presented a  $\tau_{390}$  grouped below 1.5 ns, whereas the other two samples presented much higher  $\tau_{390}$  values. The variance test on the group samples showed that the cortex  $\tau_{390}$  was significantly lower relative to the tumor  $\tau_{390}$  ( $P < 0.001$ ). The white matter  $\tau_{390}$  was also significantly lower than the tumor  $\tau_{390}$  ( $P < 0.008$ ). Except for one sample, all  $\tau_{460}$  values from the cortex sites were below 0.8 ns, whereas for the tumor sites the values were above 0.8 ns. In the case of the white



a)



b)



c)

**Figure 2.** Representative time-resolved fluorescence spectra of: (a) GBM, (b) normal cortex, and (c) normal white matter.

matter spectra, the  $\tau_{460}$  grouped below 1 ns. The variance test demonstrated that the cortex  $\tau_{460}$  was significantly lower relative to the tumor  $\tau_{460}$  ( $P < 0.03$ ). The white matter  $\tau_{460}$  was also significantly lower than the tumor  $\tau_{460}$  ( $P < 0.03$ ). The lifetime reproducibility for the five consecutive measurements acquired at 395 nm was within 0.3–15% of the mean value (median value 7%), whereas that at 460 nm was within 3–15% (median of 7.5%).

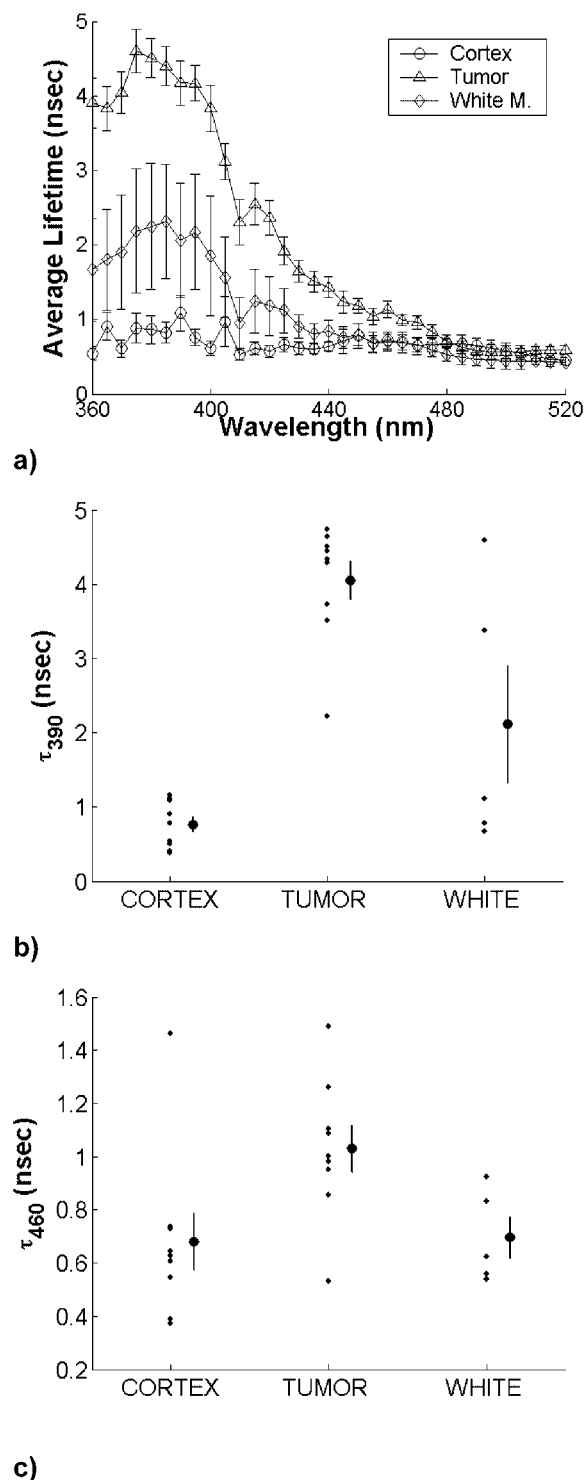


**Figure 3.** (a) Average lifetime of GBM, cortex and white matter. Results are depicted as mean  $\pm$  standard error of the data from each independent measurement. (b) The average lifetime values at 390 nm ( $\tau_{390}$ ) for each tissue type (five consecutive measurements). (c) The average lifetime values at 390 nm ( $\tau_{460}$ ) for each tissue type (five consecutive measurements). For (b) and (c) results are shown as mean of the five consecutive measurements  $\pm$  standard error of the mean.

## DISCUSSION

The time-resolved fluorescence spectroscopy studies in this small group of patients have demonstrated that lifetime fluorescence data provide a means of discrimination between neoplastic and normal brain tissue. The fluorescence lifetime information complements the conventional time-integrated (steady-state) techniques and enables a better understanding of the kinetics of the biochemical and physiological processes occurring in brain tissue across their emission spectra.

A very limited number of studies have reported the time-resolved spectra of brain tumors (19,20). Our findings suggest that the fluorescence lifetime of brain tissue is both tissue type dependent and wavelength dependent. Overall, the radiative lifetime of brain tumor tissue (GBM) is longer when compared with normal white matter and cortex and varies significantly with the emission wavelength. The fluorescence is long lived at wavelengths below 390 nm (lasting for more than 30 ns) and short lived at wavelengths around 460 nm (lasting for less than 15 ns), suggesting that two distinct fluorophores are likely to contribute to GBM emission.

We considered the possible contribution of increased scattering events as an explanation for the long fluorescence lifetime in GBM. Consequently, we investigated how optical properties of distinct types of brain tissue affect the propagation of the laser excitation pulse (21). We reported that the long-lived fluorescence at blueshifted wavelengths in tumor tissue may be due to the presence of a fluorophore with intrinsically long radiative lifetime and cannot be completely explained by an eventual distortion of the pulse width due to high scattering in the tissue. Within the temporal resolution of our instrumental apparatus, brain tissue scattering does not appear to affect the temporal profile of the measured time-resolved reflected laser pulse. The origin of this long-lived fluorescence emission, however, needs to be further investigated and is the subject of ongoing studies in our laboratory.

The short-lived fluorescence ( $\sim 1$  ns lifetime) at 460 nm corresponds to reduced nicotinamide adenine dinucleotide (phosphate) (NAD(P)H) emission and is in agreement with the steady-state studies. An interesting finding is the higher lifetime values of GBM ( $\tau_{460} \sim 1.1$  ns lifetime) when compared with normal cortex and white matter ( $\tau_{460} \sim 0.7$  ns lifetime). These lifetime values at 460 nm suggest that GBM fluorescence is likely dominated by the bound form of NAD(P)H fluorescence ( $\tau_{\text{NAD(P)H}}: 1\text{--}5$  ns) (12), whereas the normal tissue emission is related to the free form of NAD(P)H ( $\tau_{\text{NAD(P)H}}: 0.35\text{--}5$  ns) (12) emission. However, these results seem to be in opposition to results recently reported by Croce *et al.* (7), who suggested that free NAD(P)H is favored in tumors and compared their findings with a previously reported bound-free NAD(P)H ratio found in various cell lines (22). For a complete understanding and more extended comparison with these early findings, fluorescence lifetime measurements *in vivo* are needed. The *in vivo* studies will account for the metabolic function of mitochondrial enzymes that affects the NAD(P)H binding sites (23).

Spectral emission of human brain tumors, white matter and cortex, measured both *ex vivo* and *in vivo*, has been reported by a few research groups (7–9,11). Excitation wavelengths include 337 nm (9), 366 and 405 nm (7), and 360, 440 and 490 nm (8). The time-integrated spectra of white matter and cortex described by our study are in agreement with the emission spectra reported by the research groups that used 337 nm for excitation (9). They report emission characterized by a broad spectrum (360–550 nm range), modulated by a valley at 415 nm corresponding to hemoglobin absorption. For

460 nm emission, the fluorescence intensity at 460 nm of normal brain tissue was reported to be greater than that of the primary brain tumors (7–9). As reported earlier (7,8), the most likely fluorophore representing the 460 nm emission is the (NAD(P)H) in both free and bound form. The concentration of NAD(P)H was shown to vary between normal and malignant tissue. Our results confirm the early findings by displaying a significant decrease in the intensity at about 460 nm in tumor relative to normal tissue. However, in the current studies, the GBM fluorescence emission was found to be significantly reduced at longer wavelengths when compared with the blueshifted emission wavelengths, and virtually no peak emission was observed around 460 nm. Overall, our results showed that GBM is characterized by an intense fluorescence emission below 390 nm. These findings are different from those reported by Lin *et al.* (9), who described a main peak emission at 460 nm in glioblastoma and only a very weak fluorescence emission below 390 nm. The different sets of long pass filters placed in front of the spectrograph (two 360 nm filters in the previous study and 345 nm in our study) to eliminate the reflected laser could explain this discrepancy. The 345 nm allows the transmission of wavelengths above 360 nm more efficiently. Moreover, the fluorescence spectral shape was shown to vary with the storage method (8). The tumor specimens in the early studies were snap frozen and stored at  $-70^{\circ}\text{C}$ , whereas here they were investigated immediately after excision.

Although *ex vivo* measurements can demonstrate the potential for distinguishing tissues with distinct pathologies, care needs to be taken when interpreting such results. Both biochemical and metabolic properties of tissues may be considerably different *ex vivo* and *in vivo*. Because blood content and oxidation state are different, the NAD(P):NAD(P)H ratio is likely different *in vivo* when compared with *ex vivo* conditions. Differences between the emission spectra measured *in vivo* and *ex vivo* in healthy and diseased brain tissues have been reported (8). The tissue preservation and storage, moreover, may significantly affect the fluorescence properties of the *ex vivo* samples (8). To address this, we have recently developed a clinically compatible fluorescence lifetime spectroscopy system, instrumentation (24) and analytical methods (18). Clinical studies are currently being conducted at the Cedars-Sinai Medical Center using this system to measure the fluorescence lifetime of brain tissue intraoperatively. Very recent experiments (L. Marcu, unpublished data) performed intraoperatively in humans showed that the fluorescence lifetime of a brain tumor measured *in vivo* is shorter when compared with that measured in the same sample *ex vivo* postexcision. This suggests that metabolic or biochemical transformation (or both) after tumor removal may influence the fluorescence lifetime of brain tissue. This could explain the long-lived fluorescence observed in the GBM sample. Further *in vivo* studies will allow a direct comparison between *ex vivo* and *in vivo* investigations and complement the existing steady-state fluorescence spectroscopy studies on brain tissue by enabling analysis of the time-dependence of fluorescence emission.

This study is limited to the variability observed in brain specimens from seven patients. Only highly malignant brain tumors, glioblastomas, were considered. Additional studies are required to increase the knowledge of the spectroscopic features likely to be detected in lower-grade gliomas as well as within a single GBM specimen. It is well documented that gliomas display a broad range of histopathologic features including mitotically active cells, vascular proliferation, nuclear atypia and areas of necrosis. Indeed, increasingly, it is clear that the variability in phenotype and biological behavior of gliomas is a function of genomic and

proteomic variability (25). Fluorescence signals, which are determined by biochemical content and metabolic status, would be expected to vary in histologically heterogeneous tumors such as GBM. Nevertheless, the development of spectroscopic techniques capable of differentiating infiltrating tumors from adjacent normal surrounding tissue would be a considerable advance in diagnosing and detecting gliomas in an intraoperative setting.

In summary, these studies demonstrate that the use of fluorescence lifetime not only improves the specificity of fluorescence measurements but also allows a more robust evaluation of data collected from brain tissue. Combined information from both spectral- and time-domain can improve the diagnostic value of fluorescence measurements. Although further measurements *in vivo* are necessary to confirm and to provide a more detailed knowledge of the optimal fluorescence-derived parameters for distinguishing tumor from normal brain tissue, this study establishes the foundation for such intraoperative investigations.

*Acknowledgements*—This work was supported by the Whitaker Foundation. The authors thank Thanassis Papaioannou, Dr. Smita Garde and Mark Sedrak for their help with experimental work.

## REFERENCES

- Hess, K. R. (1999) Extent of resection as a prognostic variable in the treatment of gliomas. *J. Neurooncol.* **42**, 227–231.
- Matthews, P. M., M. Wylezinska and T. Cadoux-Hudson (2001) Novel approaches to imaging brain tumors. *Hematol. Oncol. Clin. North Am.* **15**, 609–630.
- Nimsky, C., O. Ganslandt, H. Kober, M. Buchfelder and R. Fahlbusch (2001) Intraoperative magnetic resonance imaging combined with neuronavigation: a new concept. *Neurosurgery* **48**, 1089–1091.
- Wagnieres, G. A., W. M. Star and B. C. Wilson (1998) *In vivo* fluorescence spectroscopy and imaging for oncological applications. *Photochem. Photobiol.* **68**, 603–639.
- Bigio, I. J. and J. R. Mourant (1997) Ultraviolet and visible spectroscopies for tissue diagnostics: fluorescence spectroscopy and elastic-scattering spectroscopy. *Phys. Med. Biol.* **42**, 803–814.
- Ramanujam, N. (2000) Fluorescence spectroscopy of neoplastic and non-neoplastic tissues. *Neoplasia* **2**, 89–117.
- Croce, A. C., S. Fiorani, D. Locatelli, R. Nano, M. Ceroni, F. Tancioni, E. Giombelli, E. Benericetti and G. Bottiroli (2003) Diagnostic potential of autofluorescence for an assisted intraoperative delineation of glioblastoma resection margins. *Photochem. Photobiol.* **77**, 309–318.
- Chung, Y. G., J. A. Schwartz, C. M. Gardner, R. E. Sawaya and S. L. Jacques (1997) Diagnostic potential of laser-induced autofluorescence emission in brain tissue. *J. Korean Med. Sci.* **12**, 135–142.
- Lin, W. C., S. A. Toms, M. Motamedi, E. D. Jansen and A. Mahadevan-Jansen (2000) Brain tumor demarcation using optical spectroscopy; an *in vitro* study. *J. Biomed. Opt.* **5**, 214–220.
- Poon, W. S., B. Ch, K. T. Schomacker, T. F. Deutsch and R. L. Martuza (1992) Laser-induced fluorescence: experimental intraoperative delineation of tumor resection margins. *J. Neurosurg.* **76**, 679–686.
- Lin, W. C., S. A. Toms, M. Johnson, E. D. Jansen and A. Mahadevan-Jansen (2001) *In-vivo* brain tumor demarcation using optical spectroscopy. *Photochem. Photobiol.* **73**, 396–402.
- Lakowicz, J. R. (1999) *Principles of Fluorescence Spectroscopy*. Plenum Press, New York.
- Das, B. B., F. Liu and R. R. Alfano (1997) Time-resolved fluorescence and photon migration studies in biomedical and model random media. *Rep. Prog. Phys.* **60**, 227–292.
- Cubeddu, R., D. Comelli, C. D'Andrea, P. Taroni and G. Valentini (2002) Time-resolved fluorescence imaging in biology and medicine. *J. Phys. D* **35**, R61–R76.
- Glanzman, T., J. P. Ballini, H. van den Bergh and G. Wagnieres (1999) Time-resolved spectrofluorometer for clinical tissue characterization during endoscopy. *Rev. Sci. Instrum.* **70**, 4067–4077.
- Marcu, L., M. Fishbein, J. M. Maarek and W. S. Grundfest (2001) Discrimination of lipid-rich atherosclerotic lesions of human coronary

- artery by time-resolved laser-induced fluorescence spectroscopy. *Atheroscler. Thromb. Vasc. Biol.* **21**, 1244–1250.
17. Papaioannou, T., N. W. Preyer, Q. Fang, A. Brightwell, M. Carnohan, G. Cottone, R. Ross, L. R. Jones and L. Marcu (2004) The effect of fiber-optic probe design and probe-to-target distance on diffuse reflectance measurements of turbid media: an experimental and computational study at 337 nm. *Appl. Opt.* **43**, 2846–2860.
  18. Jo, J. A., Q. Fang, T. Papaioannou and L. Marcu (2004) Fast model-free deconvolution of fluorescence decay for analysis of biological systems. *J. Biomed. Opt.* **9**(4), 743–752.
  19. Anderson-Engels, S., J. Johansson, K. Svanberg and S. Svanberg (1991) Fluorescence imaging and point measurements of tissue: applications to the demarcation of malignant tumors and atherosclerotic lesions from normal tissue. *Photochem. Photobiol.* **53**, 807–814.
  20. Marcu, L., R. C. Thompson, S. Garde, M. Sedrak, K. L. Black and W. H. Yong (2002) Time-resolved fluorescence spectroscopy of primary human brain tumors. *Optical Biopsy IV, SPIE Proc.* **4613**, 183–187.
  21. Butte, P. V., K. Vishwanath, B. K. Pikul, M. A. Mycek and L. Marcu (2003) Effects of tissue optical properties on time-resolved fluorescence measurements from brain tumors: an experimental and computational study. *Advanced Biomedical and Clinical Diagnostic Systems, SPIE Proc.* **4955**, 600–608.
  22. Salmon, J. M., E. Kohen, P. Viallet, J. G. Hirscheberg, A. W. Wouters, C. Kohen and B. Thorell (1982) Microspectrofluorometric approach to the study of free/bound NAD(P)H ratio as metabolic indicator in various cell types. *Photochem. Photobiol.* **36**, 585–593.
  23. Meixensberger, J., B. Herting, W. Roggendorf and H. Reichmann (1995) Metabolic patterns in malignant gliomas. *J. Neurooncol.* **24**, 153–161.
  24. Fang, Q., T. Papaioannou, J. A. Jo, R. Vaitha, K. Shastry and L. Marcu (2004) Time-domain laser-induced fluorescence spectroscopy apparatus for clinical diagnostics. *Rev. Sci. Instrum.* **75**, 151–162.
  25. Sehgal, A. (1998) Molecular changes during the genesis of human gliomas. *Semin. Surg. Oncol.* **14**, 3–12.